



## Integration of a UHF Fractal Antenna into a 1U CubeSat for Low-Earth Orbit Mission

---

Raynell Inojosa, Celso Co and Mengu Cho

EasyChair preprints are intended for rapid dissemination of research results and are integrated with the rest of EasyChair.

March 5, 2023

# Integration of a UHF Fractal Antenna into a 1U CubeSat for Low-Earth Orbit Mission

Raynell A. Inojosa<sup>1,2,3</sup>, Celso B. Co<sup>2</sup>, and Mengu Cho<sup>3</sup>

<sup>1</sup>Spacecraft Payload and Communications Systems Development Division, Philippine Space Agency

<sup>2</sup>Graduate School of Engineering, Batangas State University, Philippines

<sup>3</sup>Laboratory of Lean Satellite Enterprises and In-Orbit Experiments, Department of Electrical and Space Systems Engineering, Kyushu Institute of Technology, Japan

rainojosa@ieee.org; raynell.inojosa@philisa.gov.ph

**Abstract.** While a number of novel patch antennas have been designed and integrated into a cube satellite (CubeSat), very few attempts have been made to exploit the self-similarity features of the so-called *fractals* in the antenna design to improve the satellite communications performance. This research work presents an initial attempt to utilize these *fractal* properties in the design of a patch antenna, adopting a geometry that allows it to be incorporated into a standard 10 cm × 10 cm × 10 cm (or 1U) CubeSat. Prior to fabrication, a preliminary design was analyzed and simulated using a commercial finite element method (FEM) solver for electromagnetic structures software, High Frequency Structure Simulator (HFSS)<sup>TM</sup>. The proposed antenna was designed at a solution frequency,  $f = 920$  MHz and resonates well from 800 MHz to 1 GHz. The antenna was fabricated on an FR4 substrate ( $t = 1.6$  mm,  $\epsilon_r = 4.3$ , and  $\tan\delta = 0.02$ ) of size  $0.2\lambda \times 0.2\lambda$ . Comparison of the simulated and measured results showed a good agreement in terms of reflection coefficient and voltage standing wave ratio (VSWR) of the proposed antenna at the frequency of interest. For comparison, a commercial off-the-shelf (COTS) antenna was also characterized and measured. The measured peak gain of the proposed *fractal* antenna is at 3.148 dBi as confirmed by the radiation pattern results. It also exhibits a reflection coefficient of -26.110 dB, a VSWR of 1.104, and a wide bandwidth (BW) across the ultra-high frequency (UHF) band. This type of antenna has the potential to provide a reliable link between a CubeSat and a ground sensor terminal (GST) as confirmed by the long-range communication tests. The proposed *fractal* antenna is expected to meet the satellite data rate requirement of a CubeSat-based Internet of Things (IoT) for low-earth orbit (LEO) mission.

**Keywords:** cube satellite, *fractal* geometry, satellite antenna

## 1 Introduction

### 1.1 Cube Satellite (CubeSat)

There is a rapid advancement in satellite communications to employ a tiny cube-shaped small satellite, known as nanosatellite or cube satellite (CubeSat) as secondary payload in a launch vehicle and deployed in low-earth orbit (LEO) mission due to its low cost,

relatively fast development, and smaller space requirement for launching. Various CubeSat missions are launched into space for different applications, such as space education, space tethers, for commercial sectors and for remote sensing like weather forecasting, natural disaster monitoring, maritime tracking, and multispectral earth imaging [1-2].

Generally, the effectiveness of a satellite communications system depends on the link budget estimates, and one of the key components that is accounted to determine this is the antenna performance [3]. For internet of things (IoT) system based on CubeSat, the key feature that impacts the antennas is the link to the ground sensor terminal (GST). Therefore, the antenna should ensure a communication link between the CubeSat and the GST to support the required data rate. Also, antennas are utilized to control and monitor the satellite's health parameters. For small satellites, only a limited amount of space is allocated to the antennas. Hence, it is important to incorporate low-profile antennas to potentially reduce the volume of the satellite or allow for more space to be used for cameras, solar panels, and other payloads [4]. As a result, many antenna design engineers and researchers performed prior studies to implement various antenna architectures while considering the antenna size, CubeSat standardized structure, and the operating frequency.

## **1.2 Antennas for CubeSat**

For small satellite applications, various types of antennas (e.g., deployable, inflatable, microstrip wire) have been utilized for both the uplink and downlink communications [5]. However, these types of antennas often come with a deployment complexity, which could become the point of failure. In some instances, deployable failures can result in a total or partial loss of the spacecraft and/or the mission. To address this, printed antennas are used due to their simple and easy integration into nanosatellites and their high design flexibility [6-7]. Using the conventional printed circuit board (PCB) techniques, these antennas can be simply fabricated. Therefore, their low-profile characteristics make them excellent candidates for low-earth orbit CubeSat integration.

However, a challenging task is to design printed antennas on the CubeSat's limited surface area and allow them to resonate at relatively large wavelengths. As a result, fractal antennas have been recently investigated as the primary radiating structure for small satellites [8-10]. The geometry of fractal antennas is created by successively iterating a generator shape to a simple basis shape [11]. In the 1970s, the mathematical concepts of fractals were studied by Benoit B. Mandelbrot and were commonly defined by their self-similarity features where small regions of the geometry replicate the overall geometry on a miniaturized scale. This property of fractals is interpreted as a measure of the space-filling properties and complexity of its shape [12-13].

## **1.3 Some Fractal Antennas for CubeSat Integration**

So far, relatively few fractal antennas have been designed and optimized for CubeSat platforms and there are limited studies that integrate fractal geometries for the amateur radio band antennas like the one studied in [8]. In this work, a fractal slot antenna at second iteration was designed for CubeSat and employed for downlink telemetry

application. This was optimized to operate at 458 MHz which exhibited a return loss of  $-16.53$  dB, a bandwidth of 22.62 MHz, and an antenna gain of 2.24 dBi.

In [9], a dual-band fractal antenna based on *Minkowski* fractal geometry was investigated for LEO applications but operates in the *L*-band and *S*-band. It has a maximum gain of 7.36 dBi and a bandwidth of around 100-150 MHz. Another type of fractal antenna was explored in [10] that resonates at the *S*-band. The antenna has an omnidirectional radiation pattern with a maximum gain of 4.39 dBi at 2.3 GHz and a reflection coefficient of  $-39.56$  dB.

Table I presents a brief survey of some CubeSat antennas adopting a fractal geometry. A summary of the key design parameters such as the gains and bandwidths are shown. The authors also confirmed whether the reported literature considers the cube satellite structure during the analysis and design.

**Table 1.** Some Fractal Antennas for CubeSat.

Reference	Antenna Specifications			
	Type of fractal antenna	Gain (dBi)	BW (MHz)	Y/N*
[8]	Fractal Slot Antenna	2.24	22.62	N
[9]	Minkowski Fractal	7.36	150	N
[10]	Koch Snowflake Fractal	4.39	190	N

\* design considers the cube satellite structure; Y – Yes, N – No

In this work, a *Sierpinski* gasket fractal [14-15] at fourth iteration is uniquely adopted as the main geometry of the patch antenna optimized at the 920 MHz band for CubeSat integration.

## 2 Methods and Procedures

### 2.1 Antenna Design and Simulation

The *Sierpinski* gasket fractal in Fig.1 was simulated in HFSS<sup>TM</sup> to design the patch geometry which resulted from the continuous removal or etching of a similar triangle patch within the larger triangle. A microstrip line was added to feed the structure and a similar fractal patch was utilized as a ground plane as this provides better antenna performance based on the parametric analysis.

For the boundary, both the ground plane and the patch were assigned to finite conductivity as defined by the HFSS software. Then, an AutoCAD *.dxf* file of a 1U CubeSat structure was imported and oriented in a manner where the patch antenna radiates into free space as shown in Fig. 2. This is to simulate the possible effects of the CubeSat structure on the antenna performance.

The geometrical transformation of this geometry generated using HFSS<sup>TM</sup> is illustrated as follows,

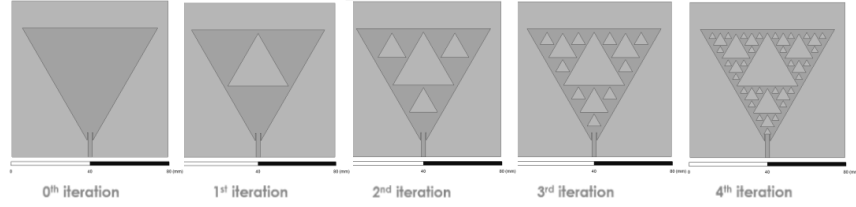


**Fig. 1.** Geometrical transformation of the fractal antenna up to fourth iteration.

The antenna was fabricated on an FR4 substrate (thickness,  $t = 1.6$  mm, relative permittivity  $\epsilon_r = 4.3$ , and loss tangent  $\tan\delta = 0.02$ ) of size  $0.2\lambda \times 0.2\lambda$ . A python code was also generated and imported to HFSS<sup>TM</sup> to easily simulate the first four iterations of the fractal antenna when performing parametric analysis.

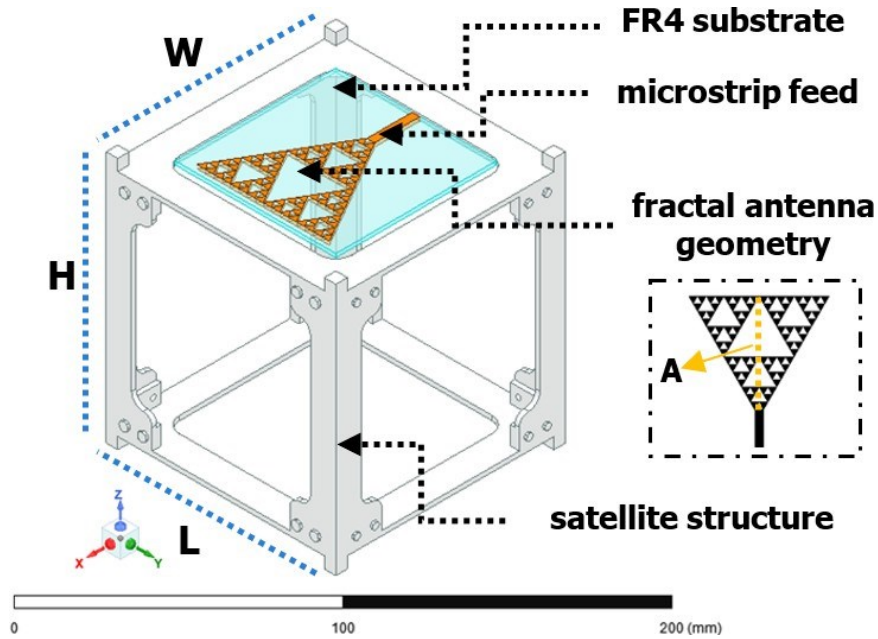


**Fig. 2.** Configuration of the simulated fractal antenna mounted on a 1U CubeSat structure ( $L=W=H=10$  cm) via HFSS<sup>TM</sup>. Fractal patch antenna dimension is  $0.15\lambda \times 0.15\lambda \times 0.006\lambda$  with the main triangle geometry altitude,  $A = 5$  cm at fourth iteration.

## 2.2 Characterization of Antenna Performance

To assess the performance of the designed fractal antenna, the simulated results of the reflection coefficient ( $S_{11}$ ), voltage standing wave ratio (VSWR), and radiation pattern

were analyzed in comparison with a conventional UHF patch as a reference. The antenna performance was characterized and simulated based on finite element method.

The reflection coefficient  $S_{11}$  is a value expressed in dB that denotes the reflection of power towards the transmitter, and also determines if there is a mismatch between the Tx port and the antenna, which is expressed as,

$$S_{11} \text{ (dB)} = 20 \log_{10}|S_{11}| = 20 \log_{10} \left| \frac{V_{reflected}}{V_{forward}} \right| \quad (1)$$

where  $V_{reflected}$  is the voltage that is reflected towards the transmitter and  $V_{forward}$  is the voltage that is incident towards the antenna. Commonly, the lower the value of  $S_{11}$ , the lower the power reflection towards the transmitter, and at the same time a better impedance matching. In that case, a maximum amount of energy is radiated by the antenna into free space. Using the CubeSat's operating frequency to plot  $S_{11}$ , the VSWR was also determined in terms of the reflection coefficient [16] by using the expression,

$$\text{VSWR} = \frac{1 + |S_{11}|}{1 - |S_{11}|} \quad (2)$$

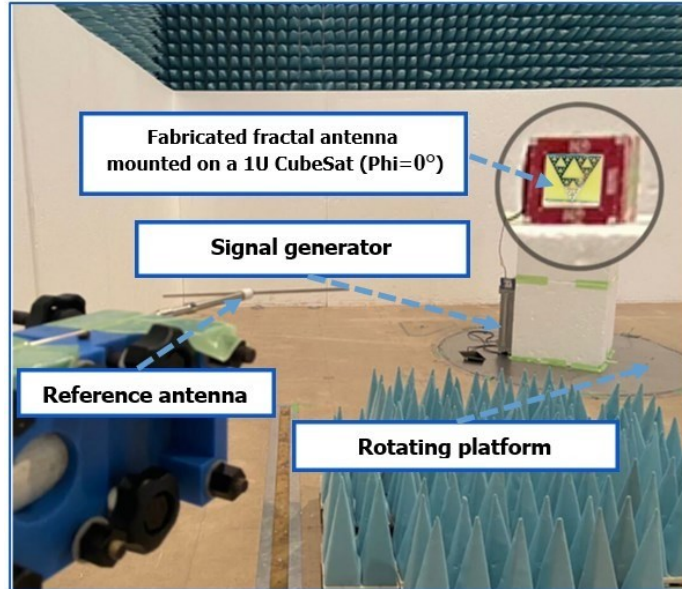
By means of simulations, the two-dimensional (2D) radiation pattern of the proposed fractal antenna was obtained to characterize the antenna response in terms of the far-field radiation. For the analysis, the co-polar plots of the radiation pattern were plotted, i.e., at  $0^\circ$  and  $90^\circ$  elevation planes.

### 2.3 Field Tests and Measurements

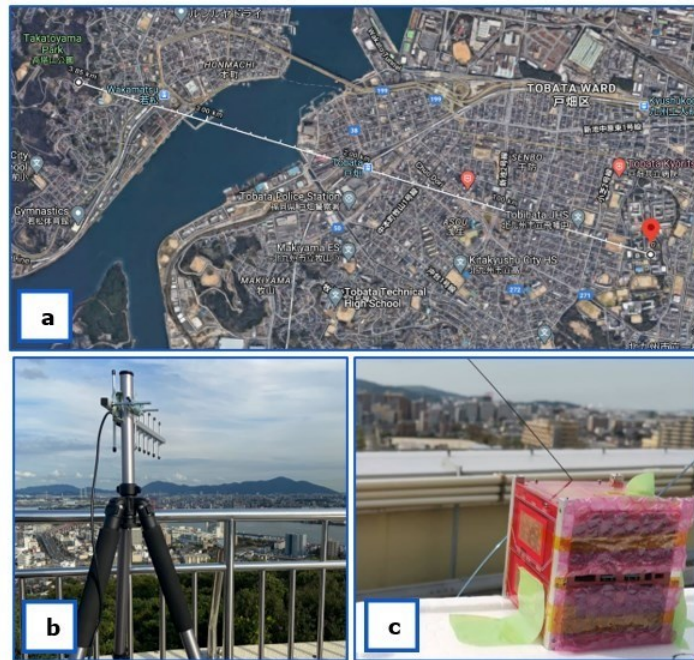
To emulate a more realistic environment, a radio anechoic chamber located at the Center for Nanosatellite Testing (CeNT) of Kyushu Institute of Technology (KyuTech) was used for measuring the radiation patterns of both the conventional and proposed fractal antenna.  $S_{11}$  and VSWR were also obtained to assess the actual antenna performance.

Figure 3 shows the configuration of the antenna far field measurement system in the anechoic chamber. The boresight gain of the antenna under test (AUT) was measured with the position controller changing the direction of the AUT in the azimuth plane. By using the external RF signal generator as the transmission source, this system was able to characterize the transmission performance of the fractal antenna mounted on a 1U nanosatellite at the specified frequency of interest.

A long-range test was also performed to verify the downlink communication between a ground sensor terminal (GST) and a satellite with the integrated fractal antenna. A flight model (FM) of a 1U CubeSat was setup at an elevated area in KyuTech while a GST was situated at the Takatoyama Park in Kitakyushu City, Japan. The distance between the transmitter and receiver was determined to be about 4 km. Figure 4 demonstrates the long-range test setup where a free space path loss (FSPL) at the operating frequency,  $f = 920$  MHz, was measured to be approximately 102 dB.



**Fig. 3.** Far-field measurement setup inside the anechoic chamber of KyuTech.



**Fig. 4.** Long-range test performed last October 2022 in Kitakyushu City, Japan: (a) distance between Tx and Rx; (b) ground station terminal,  $T_x$ ; (c) CubeSat setup with the integrated fractal antenna,  $R_x$ .

To account for the additional free space path loss of the orbital altitude, which is 138 dBm in this long-range test, a 36 dB attenuator was attached between the GST module and the transmitting antenna,  $T_x$ . The GST sent a series of data packets to the CubeSat flight model. Upon successfully receiving the data without any corrupted packets, the ground station measured the received signal. The data rate or bit rate  $R_b$  was determined by using the formula below as presented in [17],

$$R_b \text{ (bps)} = SF \times \frac{BW}{2SF} \times CR \quad (3)$$

where  $SF$  is the spreading factor,  $CR$  is the coding rate, and  $BW$  is the bandwidth.

### 3 Results and Discussions

#### 3.1 Frequency Characteristics

Figure 5 illustrates the frequency characteristics of the proposed fractal antenna at the simulated UHF band. It should be noted that the antenna might resonate well at higher frequencies above 1 GHz; however, for the context of this paper, only the nearby bands was shown for the purpose of comparing the data with the conventional patch antenna.

Across the simulated frequency range, the fractal antenna resonates perfectly with  $S_{11}$  below -10 dB. From 900 MHz above, the proposed antenna exhibits better reflection performance compared with a conventional UHF antenna. Hence, when used as a radiating structure for higher bands, the proposed antenna is expected to be more efficient. At the satellite's operating frequency,  $f = 920$  MHz, a reflection coefficient of -26.110 dB was determined.

The minimum measured  $S_{11}$  was -30.364 dB at 906 MHz while -21.425 dB was obtained at 1 GHz. The result provides an insight that the proposed fractal antenna is a good candidate for CubeSat missions that require multiband frequencies.

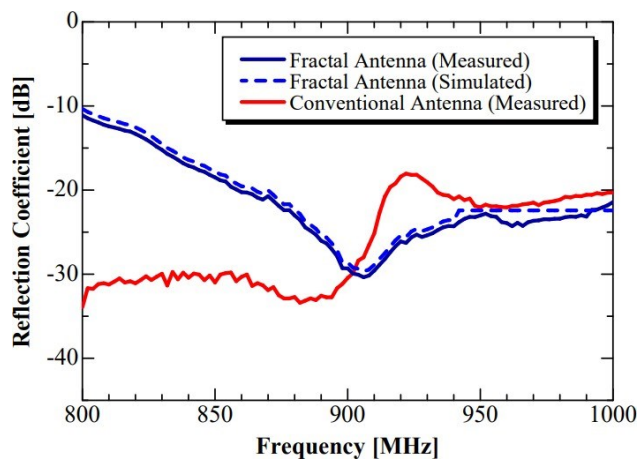


**Fig. 5.** Comparison of the reflection coefficient ( $S_{11}$ ) of the proposed fractal antenna against a conventional patch antenna within the simulated UHF band.



Figure 6 shows the comparison between the frequency characteristics of the measured and simulated VSWR of the UHF patch antennas. Similarly, the proposed fractal antenna offers better performance in terms of impedance matching at frequencies above 900 MHz in comparison with a conventional antenna. At 920 MHz, the fractal antenna's VSWR is at 1.104. Overall, the antenna's VSWR is within the acceptable value of less than 2.0.

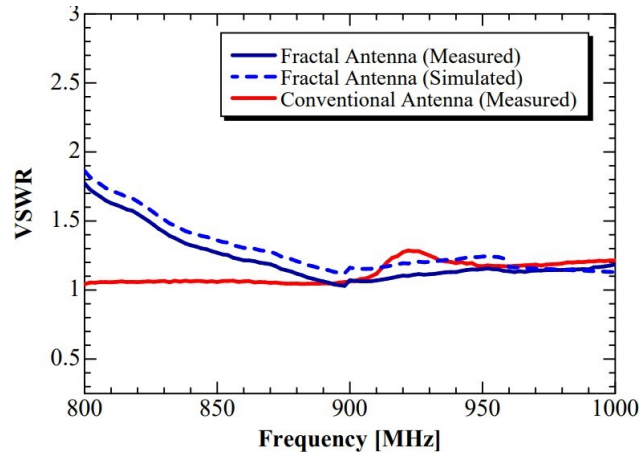


**Fig. 6.** Comparison of the VSWR of the proposed fractal antenna against a conventional patch antenna within the simulated UHF band.

### 3.2 Radiation Pattern Profile with the CubeSat Structure

The radiation pattern of the proposed fractal antenna was analyzed with a 1U CubeSat structure. The 2D radiation pattern is presented in Fig. 7. At  $\Phi = 0^\circ$ , the antenna achieved a peak gain of 4.009 dBi (simulated) and 3.148 dBi (measured) at the 920 MHz frequency band as presented.

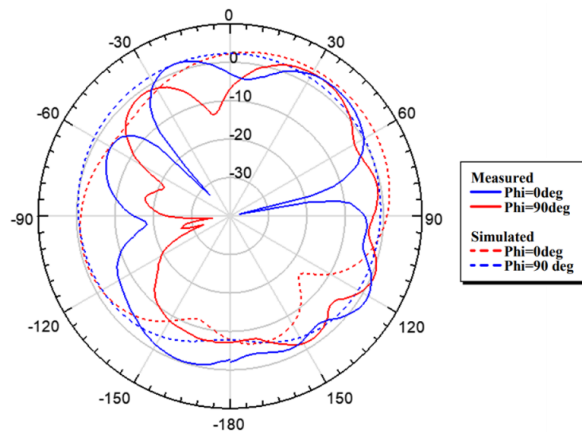


**Fig. 7.** 2D radiation pattern of the proposed fractal antenna at 920 MHz.

When the antenna was rotated at  $\text{Phi} = 90^\circ$ , the boresight gain was at 2.278 dBi (simulated) and at 2.973 dBi (measured). The simulated results show that the fractal antenna achieved a nearly omnidirectional radiation patterns in the azimuth plane. The difference between the simulated and measured data could be attributed to the fact that the simulation environment does not include the other modules of the actual CubeSat. Panel boards, electronic circuits, and other metal parts inside the CubeSat could degrade the electromagnetic performance of the antenna when it is rotated in the azimuth plane. In future designs, these structures should be considered as these components could attenuate the received signal and thereby affect the reliability of the measured results.

### 3.3 Long-range Test Results

Table II also provides the long-range test configurations using a set of predetermined transmission parameters such as spreading factor (SF), coding rate (CR), and bandwidth (BW) that create a successful downlink between the GST and the CubeSat with the mounted fractal antenna. These parameters were selected since this research work adopts a satellite-based IoT system based on the heritage of the GST and the CubeSat platform presented in [18]. Additionally, a combination of lower SF and higher BW allows higher data rates with shorter transmission distance while higher SF and lower BW provide a longer range with reduced data rate.

**Table 2.** Long-range Test Results.

Receiver Sensitivity (dBm)	Spreading Factor	Coding Rate	Bandwidth (kHz)	Data Rate (bps)
-138	12	8	31.25	30.52
-136	10	8	31.25	101.73
-138	12	8	41.70	40.72

A receiver sensitivity of -138 dBm was obtained from the field test for SF = 8 and CR = 12. For these configurations, the increase in bandwidth from 31.25 kHz to 41.70 kHz also increases the data rate as expected. With SF = 12 and CR = 8, the sensitivity is observed to decrease; however, it exhibited a data rate of 101.73 bps with a good satellite communication link.

Using the data above, a link budget analysis should be performed in future undertakings to properly design the communication system of a CubeSat. This should give an insight on how to determine power requirements, select appropriate equipment, and set up modulation parameters for signal transmission and reception. The analysis of the radio link should be done to account the gain of the proposed fractal antenna, the calculated data rate, the identified losses, and measured sensitivity among others, and to assess the link budget of the satellite communications system.

## 4 Conclusions and Future Works

This paper presents an initial attempt to design and analyze a *Sierpinski* gasket fractal antenna for low-earth orbit CubeSat integration, with a patch dimension of  $0.15\lambda \times 0.15\lambda \times 0.006\lambda$ . The proposed antenna resonates well from 800 MHz to 1 GHz with  $f=920$  MHz. The measured peak antenna gain is at 3.148 dBi as confirmed by the radiation pattern results. It also exhibits a reflection coefficient of -26.110 dB and a VSWR of 1.104 at the required operating frequency. Results confirmed that the proposed fractal antenna offers better performance against a conventional UHF antenna. This antenna also solves the challenge of designing non-deployable, low-profile, and compact antennas for the UHF band.

Other than modifying the patch size specifically for UHF band applications, the novelty of this research includes the consideration of the CubeSat frame on the antenna design. Additionally, the proposed structure consists of a ground plane with a similar geometry as the radiating patch, which has not been done yet in the context of CubeSat antennas. In future works, an investigation should be done for the optimized results for other patch geometries.

## References

1. Alam, T. et al.: Lower Ultra-High Frequency Non-Deployable Omnidirectional Antenna for Nanosatellite Communication System. In: *Nanomaterials*, Vol. 12, No. 18, p. 3143 (2022).
2. Woellert, K., Ehrenfreund, P. et al.: Cubesats: Cost-effective science and technology platforms for emerging and developing nations. In: *Advances in Space Research*, Vol. 47, Issue 4, pp. 663-684 (2011).
3. Lokman, A. et al.: A Review of Antennas for Picosatellite Applications. In: *International Journal of Antennas and Propagation* (2017).
4. Abulgasem, S., Tubbal, F., Raad, R., Theoharis, P. I., Lu, S., and Iranmanesh, S.: Antenna Designs for CubeSats: A Review. In: *IEEE Access*, Vol. 9, pp. 45289-45324 (2021).
5. Akan, V., Yazgan, E.: Antennas for space applications: A review. In: *Advanced Radio Frequency Antennas for Modern Communication and Medical Systems*, IntechOpen (2020).
6. Samsuzzaman, M., Islam, M. T., Kibria, S., and Cho, M.: BIRDS-1 CubeSat Constellation Using Compact UHF Patch Antenna. In: *IEEE Access*, Vol. 6, pp. 54282-54294 (2018).
7. Podilchak, S. K., Murdoch, A. P., and Antar, Y. M. M.: Compact, microstrip-based folded-shortened patches: PCB antennas for use on microsatellites. In: *IEEE Antennas Propagation Magazine*, Vol. 59, No. 2, pp. 88-95 (2017).
8. Simon, J. et al.: A Second-Iteration Square Koch Fractal Slot Antenna for UHF Downlink Telemetry Applications in CubeSat Small Satellites. In: *International Journal of Antennas and Propagation*, Vol. 2020, Article ID 9672959 (2020).
9. Lahcene, H. A. and Brahimi, A.: A New Design of Dual-band Fractal Antenna for LEO Applications. In: *Proceedings of the 8th International Conference on Systems and Network Communications* (2013).
10. Palacios, O. F. G., Díaz Vargas, R. E., Heraud Perez, J. A. and Correa Erazo, S. B.: S-band Koch snowflake fractal antenna for cubesats. In: *2016 IEEE ANDESCON*, pp. 1-4 (2016).

11. Singh, K. Grewal, V., and Saxena, R.: Fractal Antennas: A Novel Miniaturization Technique for Wireless Communications. In: International Journal of Recent Trends in Engineering, Vol 2, No. 5 (2009).
12. Cohen, N.: Fractal Antennas: Part 2. Communications Quarterly, Summer, pp. 53-66 (1996).
13. Mandelbrot, B. B.: The Fractal Geometry of Nature. W. H. Freeman and Company, New York, USA (1983).
14. Waqas, M., Ahmed, Z., and Ihsan, M. B.: Multiband Sierpinski fractal antenna. In: IEEE 13th International Multitopic Conference, pp. 1-6 (2009).
15. Luintel, T. and Wahid, P. F.: Modified Sierpinski fractal antenna," IEEE/ACES International Conference on Wireless Communications and Applied Computational Electromagnetics, pp. 578-581 (2005).
16. Balanis, C. A.: Modern Antenna Handbook, John Wiley & Sons (2009)
17. Augustin, A. Yi, J., Clausen, T., and Townsley, W.: A Study of LoRa: Long Range and Low Power Networks for the Internet of Things," Sensors, vol. 16, no. 9, p. 1466 (2016).
18. Lepcha, P., Malmadayalage, T.D., Örgen, N.C., Purio, M.A., Duran, F., Kishimoto, M., El Megharbel, H.A., and Cho, M.: Assessing the Capacity and Coverage of Satellite IoT for Developing Countries Using a CubeSat. In: Applied Science, Vol. 12, 8623 (2022).